

H_I line measurements of pulsars towards the Galactic Centre and the electron density in the inner Galaxy

Simon Johnston¹, Bärbel Koribalski², Joel M. Weisberg³ & Warwick Wilson²

¹QEII Fellow, School of Physics, University of Sydney, NSW 2006, Australia

²Australia Telescope National Facility, CSIRO, Epping, NSW 2121, Australia

³Carleton College, Dept. of Physics and Astronomy, Northfield, MN 55057, USA

arXiv:astro-ph/0008257v1 16 Aug 2000

27 October 2018

ABSTRACT

We have measured 21-cm absorption and emission spectra in the direction of a further 7 southern pulsars with the Parkes telescope to derive their kinematic distances and to study the interstellar medium. For the first time we have successfully obtained H_I absorption measurements for PSRs J1602–5100, J1740–3015 and J1745–3040. We have also significantly improved the sensitivity and resolution on PSRs J1600–5044, J1752–2806, and J1825–0935, whose spectra have previously been measured, and have corrected an error in the published distance to PSR J1824–1945.

Since the Frail & Weisberg summary of pulsar distances in 1990, a further 23 pulsars now have measured H_I distances, mainly through the efforts of the current group. We discuss the Taylor & Cordes electron density model in light of these new measurements and find that, although the model towards the Galactic Centre appears good, the line of sight through the Carina spiral arm is poorly fit by the model.

Key words: pulsars: general — radio lines: ISM — stars: distances

1 INTRODUCTION

We obtained neutral hydrogen (H_I) emission and absorption spectra in the direction of 7 southern pulsars to determine their kinematic distances. This paper is the third in a series on H_I observations of pulsars at the Parkes radio telescope. We refer the reader to the earlier papers by Koribalski et al. (1995; hereafter Paper I) and Johnston et al. (1996; hereafter Paper II) for a comprehensive introduction as well as a full description of the observations and data analysis.

The observations of H_I emission and absorption towards pulsars together with a rotation curve or velocity field for the Galaxy allow the derivation of lower and/or upper distance limits, depending on the distribution of H_I in the line of sight. These distance limits can be coupled with the pulsar's dispersion measure to obtain limits on the electron density along the lines of sight. From knowledge of the electron density along many lines of sight, a model can be constructed to convert dispersion measure into distance with appropriate uncertainties. The current model of Taylor & Cordes (1993) represents the synthesis of the observations to date and is widely accepted as the model of choice. However, the data poorly constrain the model towards the Galactic Centre, and the model has problems towards the Carina spiral arm as discussed in Paper II.

The pulsars described here include three within 3° of the Galactic Centre and the rest within 30° thereof. Combined

with data from four other pulsars (Weisberg et al. 1995), the current work allows a handle to be gained on the electron density in the inner Galaxy. As this is the last paper in the series, we also discuss the 23 new H_I absorption measurements since the advent of the Taylor & Cordes (1993) model and point out areas in which the model can be improved.

2 OBSERVATIONS AND DATA ANALYSIS

H_I observations towards several southern pulsars were carried out on 1994 October 5–10 using the 64-m Parkes radio telescope. The 20-cm receiver system, the correlator backend and the observing procedure were all described in Paper I. In brief, the digital correlator was configured into 2×512 channels (each with a bandwidth of 4 MHz) giving a velocity resolution of 7.8 kHz or 1.74 km s^{−1} per channel. The data were reduced off-line using standard procedures involving subtracting the 'on-pulse' spectra from the 'off-pulse' spectra with suitable normalisation (as detailed in Paper I).

Table 1 lists the pulsar parameters and details of the observing. Columns 1 and 9 list the pulsar J2000 and B1950 names. Columns 2 and 3 give the Galactic coordinates, columns 4 to 6 the pulsar period, dispersion measure and flux density, respectively. Columns 7 and 8 give the integration time in minutes and the number of time bins for each pulsar. In all cases the pulse occupied only 1 of these phase

bins (which was used to form the on-pulse spectrum) and the remaining were used for the formation of the off-pulse spectrum.

To calibrate the brightness temperature of the emission spectra we used the Kerr et al. (1986) emission survey for PSRs J1600–5044 and J1602–5100, the Burton & Liszt (1983) survey for PSRs J1740–3015, J1745–3040 and J1752–2806 and the Weaver & Williams (1974a, 1974b) survey for PSRs J1824–1945 and J1825–0935. To convert from the antenna temperatures quoted in those papers to true brightness temperatures we used a correction factor of 1.025 for Kerr et al., 1.52 for Burton & Liszt and 1.14 for Weaver & Williams. Subject to the caveats contained in those papers, we estimate the uncertainty in our brightness temperatures to be of the order of 5%.

3 RESULTS ON INDIVIDUAL SOURCES

Figure 1 shows the emission and absorption spectra for each of the 7 pulsars. Below the spectra we show the rotation curve appropriate for the longitude and latitude of the pulsar. In this paper we use an analytic expression given by the best fit model of the Galactic rotation curve from Fich, Blitz, & Stark (1989). We adopt the standard IAU parameters (Kerr & Lynden-Bell 1986) for the distance to the Galactic centre ($R_0 = 8.5$ kpc) and the solar orbital velocity ($V_0 = 220$ km s $^{-1}$). The rotation curve of the Galaxy is the azimuthally smoothed average of its velocity field and thus implicitly assumes circular orbits around the Galactic centre.

The lower and upper distance limits of pulsars can be inferred from their absorption and emission spectra, respectively. Following Frail & Weisberg (1990; Section V.a) we set the lower distance limit, D_L , from the centre of the farthest absorption feature in the spectrum and the upper distance limit, D_U , by the first emission peak above $T_B = 35$ K and beyond the most distant absorption feature. The lower limit of 35 K on the brightness temperature is a conservative approach if one wishes to be certain of detecting absorption (Radhakrishnan et al. 1972; Weisberg, Boriakoff & Rankin 1979). The simple Galactic rotation model cannot take into account the presence of random or streaming motions in the H I gas which causes departures from purely circular rotation. One must allow for errors of the order 7 km s $^{-1}$ when converting the observed velocities into distances (see, e.g., Weisberg et al. 1979; Shaver et al. 1982; Clifton et al. 1988).

For pulsars near the Galactic Centre, velocity crowding means that no useful distances can be obtained directly from the Doppler shift of the H I line. However, comparison with other objects with known distance and velocity can provide useful constraints as can the ‘peculiar’ velocity of the expanding 3 kpc arm. For all the objects discussed below we use as much information from the literature as possible when computing distance limits.

Table 2 shows the measured lower and upper velocity limits for each pulsar with the corresponding distance limits, where the distance errors are computed assuming random motions of the H I gas contribute 7 km s $^{-1}$ as described above. The electron density limits are then given by the dispersion measure (Table 1) divided by the distance limits. A discussion of the results for each pulsar is given below.

3.1 PSR J1600–5044 (B1557–50); l,b=330°.7,1°.6

Low-resolution H I absorption spectra have been obtained by Ables & Manchester (1976) and Manchester et al. (1981), but differ substantially. The differences in optical depth near –40 km s $^{-1}$ in the two spectra are discussed in Deshpande et al. (1992) who claim this as evidence for small-scale ISM structure. The pulsar is close on the sky to PSR J1602–5100 discussed below.

Our measurements show, with much improved spectral resolution, strong (> 35 K) H I emission between –91 km s $^{-1}$ and +30 km s $^{-1}$. Several narrow absorption features are visible throughout this range in addition to an astonishing absorption feature at –105 km s $^{-1}$. It has an optical depth of 0.94 against an emission feature which has a temperature of only 10 K! It is unusual to see such deep absorption in a relatively weak emission feature at this longitude although similar absorption is sometimes seen against the 3-kpc arm in the inner Galaxy. The data yield a spin temperature of about 20 K, indicating that the absorption cloud is unusually cold. The H I emission survey of Kerr et al. (1986) reveals nothing unusual in the vicinity. The brightness temperature of the emission rises steeply towards the Galactic Plane at this velocity, peaking near 100 K. One possibility is that the absorption could be associated with the small, cold, high density clouds which were recently detected in large numbers in an infra-red galactic plane survey (Egan et al. 1998). However, these clouds are predominantly molecular (Carey et al. 1998) and it is unclear how much neutral atomic hydrogen would exist there.

The distance corresponding to this feature is at 6.4 ± 0.5 kpc which we assign as our lower distance limit. This is somewhat more conservative than Frail & Weisberg (1990) who assign the tangent point distance of 7.4 ± 1.1 kpc as the lower distance limit based on critical analyses of the spectra of Ables & Manchester (1976) and Manchester et al. (1981). At positive velocities, we might expect to see some absorption towards the emission peak at +29.7 km s $^{-1}$, though its brightness is only 33 K. From the lack of any significant absorption here we infer an upper distance limit of 18.2 ± 1.2 kpc. Although the emission temperature does not (quite) reach our 35 K cutoff criterion, the relatively small noise in the absorption spectrum strengthens our argument that the lack of observed absorption supports the quoted upper limit.

Caswell et al. (1975) observed H I towards a number of (Galactic) sources between longitudes 328° and 332°. All these are closer to the Galactic plane than PSR J1600–5044 and in all cases emission temperatures of ~ 100 K are seen at –105 km s $^{-1}$. The closest supernova remnant to the pulsar is SNR 330.2+1.0 (Caswell et al. 1983) but unfortunately it has not been observed in H I nor has there been any detection of maser lines associated with it (Green et al. 1997).

3.2 PSR J1602–5100 (B1558–50); l,b=330°.7,1°.3

Frail & Weisberg (1990) discuss an unpublished low-resolution spectrum for this pulsar by Manchester. They note the apparent absorption seen near the tangent point velocity of –110 km s $^{-1}$. At this velocity the emission temperature is only 12 K. However, assuming the absorption is real they assign the tangent point distance of 7.4 ± 1.1 kpc as a *lower* limit.

The emission spectrum is very similar to that of PSR J1600–5044 (described above) with strong H_I emission between -90 and $+30$ km s $^{-1}$. Our spectrum shows absorption at least up to -72 km s $^{-1}$ corresponding to a distance of 4.5 ± 0.4 kpc. There is no absorption seen against the reasonably bright feature at -90 km s $^{-1}$. Gas at this velocity can either be on the near or far side of the tangent point, hence we set the upper limit to be beyond the tangent point at a distance of 9.4 ± 0.4 kpc. However, we also have a hint of absorption near -110 km s $^{-1}$ as in the Manchester spectrum. This feature has an optical depth of 0.36 (4.6σ). Given that we see strong absorption at -105 km s $^{-1}$ in PSR J1600–5044 (only 20 arcmin distant) against a similarly low temperature cloud we assign a lower distance limit at the tangent point (7.4 ± 0.5 kpc).

There are 2 known H_{II} regions located near the pulsar and significantly off the Galactic plane. G331.354+1.072 has a recombination line velocity of -79 km s $^{-1}$ and G331.360+0.507 has a velocity of -46 km s $^{-1}$ in both recombination lines and H₂CO (Caswell & Haynes 1987), but no independent distances are known.

3.3 PSR J1740–3015 (B1737–30); l,b=358°.3,0° PSR J1745–3040 (B1742–30); l,b=358°.6,−1°

These pulsars are only 1° apart on the sky and lie within 2° of the Galactic centre. Along this line of sight, velocity crowding is too severe to convert velocity to distance. However, the presence of the 3 kpc arm at a velocity of -60 km s $^{-1}$ (see Burton & Liszt 1983) helps to constrain the distance.

Both pulsars show similar emission profiles. Strong H_I emission extends from -20 km s $^{-1}$ to $+20$ km s $^{-1}$ and there is a dip in the brightness temperature due to self-absorption from a local cloud (Crutcher & Lien 1984) at a velocity of $+8$ km s $^{-1}$. Towards both pulsars, emission is seen from the 3 kpc arm at -60 km s $^{-1}$ although the brightness temperature is significantly less than 30 K in the case of PSR J1745–3040 and only ~ 30 K for PSR J1740–3015.

The absorption profiles of the pulsars differ in that absorption with an optical depth of ~ 0.5 is seen at -15 km s $^{-1}$ towards PSR J1740–3015 but not towards PSR J1745–3040. No absorption is seen against the 3 kpc arm in either pulsar. Dickey et al. (1983) and Garwood & Dickey (1989) show H_I spectra towards 3 background sources (1739-298, 1741-312 and 356.905+0.082) all less than 2° from the pulsars. Absorption at -15 km s $^{-1}$ and against the 3 kpc arm is clearly seen. SNR G357.7–0.1 (MSH 17–39; the Tornado) shows similar absorption characteristics - deep absorption features from $+20$ to -15 km s $^{-1}$ and absorption at the location of the 3 kpc arm at -60 km s $^{-1}$ (Radhakrishnan et al. 1972). This remnant is located beyond the 3 kpc arm, and possibly beyond the Galactic Centre (Frail et al. 1996). The other complex of interest in this region of sky contains the SNR G359.1–0.5, the ‘Mouse’ (G359.2–0.8) and the ‘Snake’ (G359.1–0.2). H_I observations of this whole area by Uchida et al. (1992), show that the Snake and the SNR lie beyond the 3 kpc arm but the Mouse shows no absorption against the gas in the arm and is presumed to be a foreground object.

Given the evidence above, we should certainly see absorption against PSR J1740–3015 if it were located behind

the 3 kpc arm, and we do not. Following Weisberg et al. (1995), therefore, we assign the 3 kpc arm at 5.5 ± 0.6 kpc as the upper distance limit. Given that absorption is seen against the emission at -15 km s $^{-1}$ we conclude that this feature lies in front of the 3 kpc arm but at an unknown distance. As PSR J1745–3040 does not show absorption at -15 km s $^{-1}$ in spite of a high emission temperature we conclude that it must be in front of the arm, in front of PSR J1740–3015 and also in front of the -15 km s $^{-1}$ feature. Unfortunately, the lack of any further kinematic information in this region forces us to assign an upper distance limit of 5.5 ± 0.6 kpc for this pulsar also.

The upper limits derived are consistent with the dispersion measure distances to the pulsars and we note also that PSR J1745–3040 has a lower dispersion measure than PSR J1740–3015 as expected if it is closer.

Saravanan et al. (1996) also observed both of these pulsars. Their absorption spectrum on PSR J1740–3015 is similar to ours, although ours has less noise in spite of a slightly shorter integration time. We also do not see any absorption against the weak emission feature at -180 km s $^{-1}$ that is visible in their figure nor would any absorption be expected at this velocity given that the pulsar is closer than the 3-kpc arm. (Saravanan et al. do not set any distance limits on the basis of this feature.) For PSR J1745–3040, our integration time was longer than theirs and our spectrum less noisy. Although the absorption spectra appear different, given the relatively high noise levels in the spectra they appear to be consistent at the 3σ level.

3.4 PSR J1752–2806 (B1749–28); l,b=1°.5,−1°

This pulsar was one of the first discovered (Turtle & Vaughan 1968). A low resolution H_I absorption spectrum by Guelin et al. (1969) did not clearly show absorption, but a Gordon et al. (1969) spectrum with a resolution of 3.8 km s $^{-1}$ shows a single absorption feature at $+9$ km s $^{-1}$, coincident with the self-absorption feature in the emission spectrum.

This pulsar scintillates rather strongly through the 4 MHz band and, in contrast to the other pulsars in this sample, we fitted the absorption profile baseline (excluding the channels of interest) with a 7th order polynomial to remove the effects of the scintillation. Our data show three clear absorption features at velocities of $+4.9$, $+8.2$ and $+14.8$ km s $^{-1}$. The feature at $+8.2$ km s $^{-1}$ is exactly coincident with the self-absorption feature in the emission profile and is the same as that seen by Gordon et al. (1969). We note that if our spectrum is smoothed to the same velocity resolution as that of Gordon et al., the three lines blend together into a single feature. The features at both $+5$ and $+9$ km s $^{-1}$ are due to a cold cloud at a distance of 125 pc (Crutcher & Lien 1984) and Frail & Weisberg (1990) adopted this as the lower limit to the pulsar’s distance.

We note, however, several other objects in this region with similar velocities. The H_{II} region RCW 142 (G0.55–0.85) has a recombination line velocity of $+13.3$ km s $^{-1}$, an OH maser at $+16.8$ km s $^{-1}$ and H₂CO velocities of $+15.6$ and $+20.8$ km s $^{-1}$ (Gardner & Whiteoak 1975). Two nearby reflection nebulae (RCW 137 and 141) have H α velocities of $+12.2$ and $+9.6$ km s $^{-1}$, respectively (Georgelin & Georgelin 1970). Finally, the OH/IR star IRAS 17482–2824 (Galactic

coordinates $1.0, -0.83$) has a maser velocity of $+10 \text{ km s}^{-1}$ and a photometrically derived distance of 1.2 kpc (Lepine, Ortiz & Epchtein 1995). It is appealing to claim that because we see absorption beyond $+10 \text{ km s}^{-1}$ in our spectrum we could raise the lower distance limit to the pulsar to 1.2 kpc . However, the peculiar motion of the OH/IR star is uncertain and the large spread in velocities of the features in RCW 142 forces us to adopt a cautious approach and hence we leave the lower distance limit as 0.125 kpc . If distances were measured to any of the RCW regions listed above the distance limit could be significantly improved.

3.5 PSR J1824–1945 (B1821–19); $l,b=12^\circ.3, -3^\circ.1$

Saravanan et al. (1996) observed this pulsar in $\text{H}\alpha$ and derived a lower distance limit of 2 kpc . In our spectrum $\text{H}\alpha$ in emission extends from $+5$ to $+35 \text{ km s}^{-1}$. $\text{H}\alpha$ absorption is seen over the same velocity range and the last absorption peak at $+26.4 \text{ km s}^{-1}$ defines the lower distance limit with $3.2 \pm 0.5 \text{ kpc}$. The lack of $\text{H}\alpha$ above 30 K beyond this point implies no upper distance limit can be set. We note that the 4σ absorption against the emission feature at $+35 \text{ km s}^{-1}$ is marginally significant. However, the low brightness temperature of this feature (25 K) and the lack of absorption at this velocity in the Saravanan et al. (1996) spectrum makes it unlikely that the absorption is real. The conversion from velocity to distance is significantly in error in Saravanan et al. (1996) and our result defines the new distance limit.

An OH/IR star IRAS 18176–1848 lies about 1° away from the pulsar, has a maser velocity of 13 km s^{-1} and a photometrically derived distance of 2.6 kpc (Lepine, Ortiz & Epchtein 1995) consistent with the above result, if we also allow for a 7 km s^{-1} component of random velocity in the maser. Gathier et al. (1986) display 21-cm absorption profiles of the planetary nebula NGC 6578 at galactic coordinates $10^\circ.8, -1^\circ.8$ and another source at $11^\circ.3, -1^\circ.6$. However, since their absorption cuts off at lower velocities than does the pulsar's, they provide no additional useful kinematic information.

3.6 PSR J1825–0935 (B1822–09); $l,b=21^\circ.5, 1^\circ.3$

Gómez-Gonzàles & Guélin (1974) obtained a low-resolution ($\Delta v \sim 13 \text{ km s}^{-1}$) $\text{H}\alpha$ spectrum towards this pulsar, from which they derive only an upper distance limit of 1.5 kpc . In our high resolution spectrum we see strong $\text{H}\alpha$ emission between zero and $+38 \text{ km s}^{-1}$. The absorption is seen only against the gas at zero velocity and hence no lower velocity limit can be set. There is no significant absorption against either the feature at $+20 \text{ km s}^{-1}$ or $+35 \text{ km s}^{-1}$. Dickey et al. (1983) observed two nearby (extragalactic) sources within $\sim 1^\circ$ of the pulsar but at slightly higher galactic latitudes. Both 1817–098 (G20.7+2.3) and 1819–096 (G21.0+2.0) show deep absorption ($\tau > 1$) out to $+35 \text{ km s}^{-1}$.

Garwood & Dickey (1989), Radhakrishnan et al. (1972) and Caswell et al. (1975) show $\text{H}\alpha$ observations to 4 other sources (G19.6–0.2, G21.5–0.9, G24.0+0.2 and G24.8+0.1) within $\sim 2^\circ$ of the pulsar. Again, deep absorption is seen out to at least $+60 \text{ km s}^{-1}$ in all the sources, although their lower galactic latitude indicates that they are not the ideal comparison sources that the first two are.

We thus assign an upper distance limit of $1.9 \pm 0.4 \text{ kpc}$ based on the lack of absorption against the emission feature at $+20 \text{ km s}^{-1}$.

4 DISCUSSION

The review of Frail & Weisberg (1990) contained 50 pulsars for which $\text{H}\alpha$ lower and/or upper distance limits had been measured. Shortly thereafter, Taylor & Cordes (1993) developed a model of the electron density distribution in the Galaxy to allow for the conversion from a pulsar's dispersion measure to its distance. Since then, 28 pulsars have been observed in $\text{H}\alpha$ of which 18 were observed for the first time and 5 had significantly different $\text{H}\alpha$ kinematic distances to those derived in older literature (Frail et al. 1993, Paper I, Weisberg et al. 1995, Paper II, Saravanan et al. 1996, this work). The pulsars mainly lie in the 4th quadrant of the Galaxy. The tangent points of three major spiral arms lie in this quadrant (in order of increasing distance from the Sun and decreasing distance from the Galactic Centre; the Carina, Crux, and Norma arms), but previous $\text{H}\alpha$ observations of pulsars were few and far between. The most recent discussion and summary of new results can be found in Weisberg (1996).

We can extend the work of Weisberg et al. (1995) in order to see how the Taylor & Cordes (1993) model matches up to the new results. Somewhat surprisingly, the distance derived by the model to 11 of the 24 pulsars lie outside the measured $\text{H}\alpha$ distances, 7 on the low side and 4 on the high side. Figure 2 displays this in graphical form. In the Figure, the pulsars are projected onto an X-Y plane with the Galactic Centre at $0,0$ and the Sun at $0,8.5$. The location of the spiral arms included by Taylor & Cordes in their model are shown on the plot as is their inner annulus of enhanced electron density. Solid diamonds represent the Taylor & Cordes (1993) dispersion measure derived positions. The solid lines indicate the range of $\text{H}\alpha$ measured kinematic positions; those with an arrow have no upper distance limit. The two pathological cases with very large DM-derived distances compared to the $\text{H}\alpha$ distance, PSRs J1056–6258 and J1801–2305, are almost certainly located behind $\text{H}\alpha$ regions which contribute substantially to the dispersion measure (Paper II; Frail et al. 1993).

It is interesting to note that for most of the Galactic Centre pulsars, the model does a reasonable job. However, very few pulsars lie beyond the expanding arm in this direction and even fewer lie on the far side of the Galactic Centre. Taylor & Cordes (1993) have made the point that this does not allow them to distinguish whether the electron density reaches a peak in an annulus at some radius from the Galactic Centre or continues increasing until the Centre.

Of the 8 pulsars between longitudes 300° and 342° (along the tangents to the Sagittarius–Carina and Scutum–Crux arms), no fewer than 6 are not well fitted by the Taylor & Cordes model and all 6 have $\text{H}\alpha$ distances *larger* than those calculated from the model. It is evident from the figure that the Taylor & Cordes model tends to assign pulsars to spiral arms because of the large electron density excess in those regions in the model, so that a relatively large range of dispersion measure corresponds to a small change in distance.

In particular the model seems to overestimate the electron density in the Sagittarius-Carina arm.

A further aid to determining distances to pulsars located behind spiral arms is to compare their scintillation speeds with their proper motions (Gupta 1995). The scintillation speed has a different distance dependence to the proper motion velocity and also depends on the location of the scattering screen (in this case presumably the spiral arm). Unfortunately not many pulsars have both scintillation and proper motion measurements. One example is PSR J1453-6413. Its dispersion measure distance of 1.8 kpc is at odds with the H_I lower limit of 2.5 kpc. If we assume the spiral arm is 1.5 kpc from Earth in this direction, then to match the scintillation speed (Johnston, Nicastro & Koribalski 1998) with the proper motion (Bailes et al. 1990) requires a pulsar distance of 3.3 kpc, consistent with the H_I lower limit. Although this is just one example (but see also McClure-Griffiths et al. 1995), it may be that towards the very clumpy regions of the spiral arms that scintillation parameters are more appropriate than dispersion measure for assigning distances to those pulsars for which H_I absorption measurements are impractical. Ideally, one requires H_I, scintillation and proper motion measurements of a large number of pulsars in order to significantly refine further the electron density model of the Galaxy.

5 CONCLUSIONS

This paper completes our analysis of H_I observations towards 22 southern hemisphere pulsars started in Papers I and II. The main results from these three papers are:

- (i) The Taylor & Cordes (1993) model does a good job in assigning distances to pulsars behind the Gum Nebula.
- (ii) As found in other studies, the H_I gas is seen at velocities forbidden by the standard Galactic rotation model along directions tangent to the Carina spiral arm.
- (iii) PSR J1709-4429, one of the few pulsars observable at TeV energies, has a well-defined H_I distance which appears to rule out the association with a nearby supernova remnant.
- (iv) At least on the near side of the expanding 3 kpc arm, the Taylor & Cordes distance model works well towards the Galactic Centre.
- (v) Dispersion measure is not necessarily a good indicator of distance when looking through the spiral arms, and modifications to the distance model appear to be necessary in the region $300^\circ < l < 345^\circ$.

ACKNOWLEDGMENTS

JMW was supported by NSF Grant AST9530710. The Australia Telescope is funded by the Commonwealth of Australia for operation as a National Facility managed by the CSIRO.

REFERENCES

Ables J. G., Manchester R. N., 1976, AA, 50, 177
 Bailes M., Manchester R. N., Kesteven M. J., Norris R. P., Reynolds J. E., 1990, MNRAS, 247, 322

Burton W. B., Liszt H. S., 1983, A&AS, 52, 63
 Carey S. J., Clark F. O., Egan M. P., Price S. D., Shipman R. F., Kuchar T. A., 1998, ApJ, 508, 721
 Caswell J. L., Haynes R. F., 1987, AA, 171, 261
 Caswell J. L., Murray J. D., Roger R. S., Cole D. J., Cooke D. J., 1975, AA, 45, 239
 Caswell J. L., Haynes R. F., Milne D. K., Wellington K. J., 1983, MNRAS, 204, 915
 Clifton T. R., Frail D. A., Kulkarni S. R., Weisberg J. M., 1988, ApJ, 333, 332
 Crutcher R. M., Lien D. J., 1984, in Kondo Y., Bruhweiler F. C., Savage B. D., eds, IAU Colloquium No. 81: The local interstellar medium. NASA CP2345, Washington, p. 117
 Deshpande A. A., McCulloch P. M., Radhakrishnan V., Anantharamaiah K. R., 1992, MNRAS, 258, 19P
 Dickey J. M., Kulkarni S. R., van Gorkom J. H., Heiles C. E., 1983, ApJS, 53, 591
 Egan M. P., Shipman R. F., Price S. D., Carey S. J., Clark F. O., Cohen M., 1998, ApJ, 494, L199
 Fich M., Blitz L., Stark A. A., 1989, ApJ, 342, 272
 Frail D. A., Weisberg J. M., 1990, AJ, 100, 743
 Frail D. A., Kulkarni S. R., Vasisht G., 1993, Nat, 365, 136
 Frail D. A., Goss W. M., Reynoso E. M., Giacini E. B., Green A. J., Otrupcek R., 1996, AJ, 111, 1651
 Gardner F. F., Whiteoak J. B., 1975, MNRAS, 171, 29P
 Garwood R. W., Dickey J. M., 1989, ApJ, 338, 841
 Gathier R., Pottasch S., Goss W., 1986, AA, 157, 191
 Georganis Y. P., Georganis Y. M., 1970, AA, 6, 349
 Gomez-Gonzalez J., Guelin M., 1974, AA, 32, 441
 Gordon C. P., Gordon K. J., Shalloway A. M., 1969, Nat, 222, 129
 Green A. J., Frail D. A., Goss W. M., Otrupcek R., 1997, AJ, 114, 2058
 Guelin M., Guibert J., Huchtmeier W., Weliachew L., 1969, Nat, 221, 249
 Gupta Y., 1995, ApJ, 451, 717
 Johnston S., Nicastro L., Koribalski B., 1998, MNRAS, 297, 108
 Johnston S., Koribalski B. S., Weisberg J. M., Wilson W., 1996, MNRAS, 279, 661 (Paper II)
 Kerr F. J., Lynden-Bell D., 1986, MNRAS, 221, 1023
 Kerr F. J., Bowers P. F., Jackson P. D., Kerr M., 1986, A&AS, 66, 373
 Koribalski B. S., Johnston S., Weisberg J. M., Wilson W., 1995, ApJ, 441, 756 (Paper I)
 Lepine J. R. D., Ortiz R., Epchtein N., 1995, AA, 299, 453
 Manchester R. N., Wellington K. J., McCulloch P. M., 1981, in Sieber W., Wielebinski R., eds, Pulsars, IAU Symposium 95. Reidel, Dordrecht, p. 445
 McClure-Griffiths N., Johnston S., Stinebring D., Nicastro L., 1998, ApJ, 492, L49
 Radhakrishnan V., Goss W. M., Murray J. D., Brooks J. W., 1972, ApJS, 24, 49
 Saravanan T. P., Deshpande A. A., Wilson W., Davies E., McCulloch P. M., McConnell D., 1996, MNRAS, 280, 1027
 Shaver P. A., Radhakrishnan V., Anantharamaiah K. R., Retallick D. S., Wamsteker W., Danks A. C., 1982, AA, 106, 105
 Taylor J. H., Cordes J. M., 1993, ApJ, 411, 674
 Turtle A. J., Vaughan A. E., 1968, Nat, 219, 689
 Uchida K., Morris M., Yusef-Zadeh F., 1992, AJ, 104, 1533
 Weaver H., Williams D. R. W., 1974a, A&AS, 17, 1
 Weaver H., Williams D. R. W., 1974b, A&AS, 8, 1
 Weisberg J. M., 1996, in Johnston S., Walker M. A., Bailes M., eds, Pulsars: Problems and Progress, IAU Colloquium 160. Astronomical Society of the Pacific, San Francisco, p. 447
 Weisberg J. M., Boriakoff V., Rankin J., 1979, AA, 77, 204
 Weisberg J. M., Siegel M. H., Frail D. A., Johnston S., 1995, ApJ, 447, 204

Table 1. Pulsar parameters and observing information

PSR (J2000)	<i>l</i>	<i>b</i>	DM (pc cm ⁻³)	Period (ms)	S ₂₀ (mJy)	T (min)	bins	PSR (B1950)
1600–5044	330°.7	1°.6	262.8	192.60	15	232	16	1557–50
1602–5100	330°.7	1°.3	169.5	864.20	6	398	32	1558–50
1740–3015	358°.3	0°.2	153.0	606.64	6	175	32	1737–30
1745–3040	358°.6	−1°.0	88.8	367.43	14	224	16	1742–30
1752–2806	1°.5	−1°.0	50.4	562.56	35	50	32	1749–28
1824–1945	12°.3	−3°.1	224.3	189.33	9	324	16	1821–19
1825–0935	21°.5	1°.3	19.9	768.97	11	427	16	1822–09

Table 2. H I kinematic distances for 7 pulsars

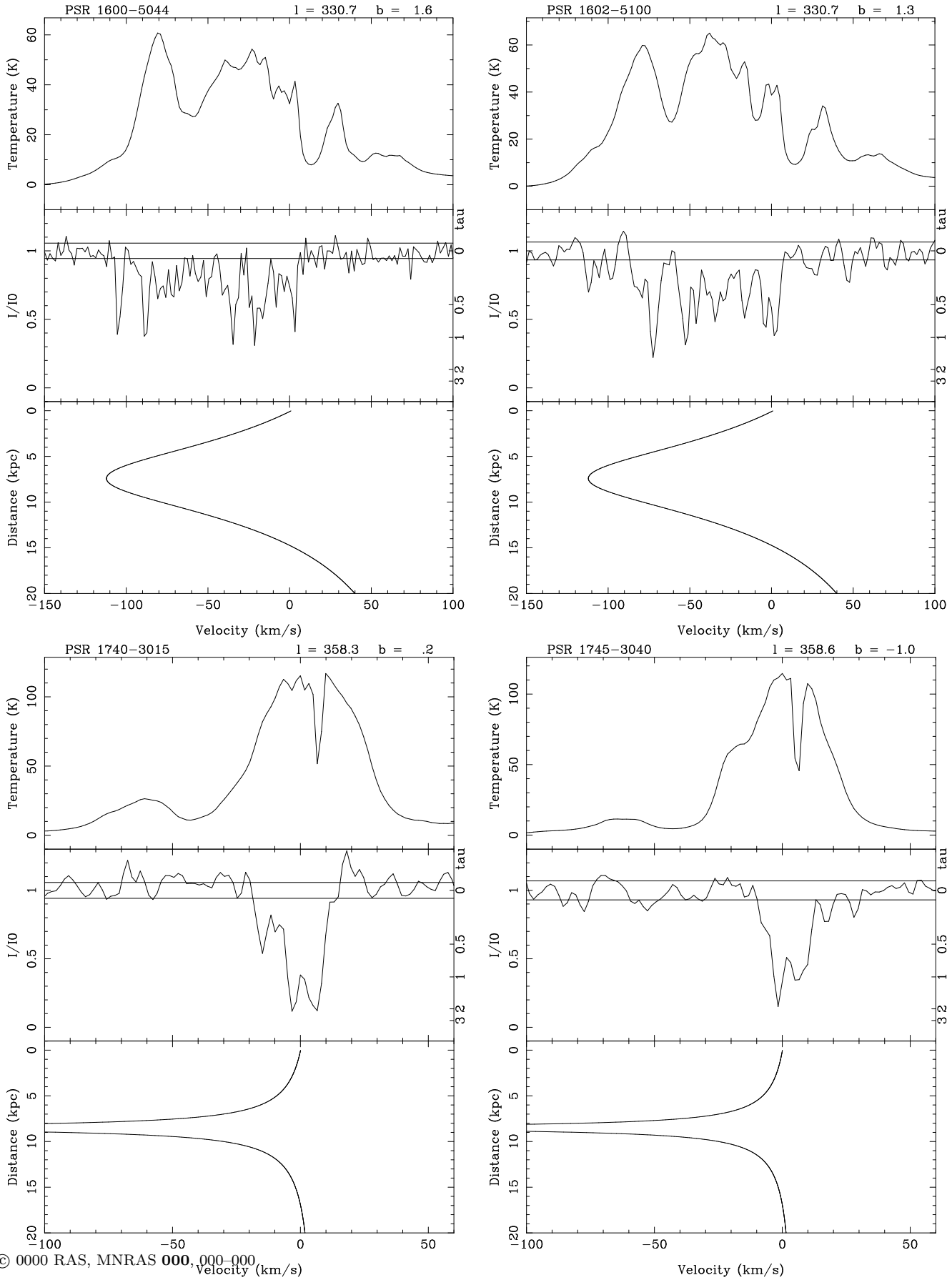
PSR (J2000)	<i>v_L</i> (km s ⁻¹)	<i>v_U</i> (km s ⁻¹)	<i>D_L</i> (kpc)	<i>D_U</i> (kpc)	<i>n_e</i> (cm ⁻³)
1600–5044	−105	+29.7	6.4±0.5	18.2±1.2	0.014 – 0.041
1602–5100	−110	−90	7.4±0.5	9.4±0.4	0.018 – 0.023
1740–3015	−14.8	−60	—	5.5±0.6	>0.028
1745–3040	—	−20	—	5.5±0.6	>0.016
1752–2806	+14.8	—	0.125	—	<0.40
1824–1945	+26.4	—	3.2±0.5	—	<0.070
1825–0935	—	+19.8	—	1.9±0.4	>0.010

Table 3. New H I distances since Frail & Weisberg (1990)

PSR (J2000)	<i>l</i> (°)	<i>b</i> (°)	<i>D_L</i> (kpc)	<i>D_U</i> (kpc)	Ref.	PSR (B1950)
0742–2822	243°.8	−2°.4	2.0±0.6	6.9±0.8	2	0740–28
0907–5157	272°.2	−3°.0	—	8.0	5	0905–51
0908–4913	270°.3	−1°.0	2.4±1.6	6.7±0.7	2	0906–49
0942–5552	278°.6	−2°.2	—	7.5±0.7	4	0940–55
1048–5832	287°.4	0°.6	2.5±0.5	5.6±0.8	4	1046–58
1056–6258	290°.3	−3°.0	2.5±0.5	2.9±0.5	2	1054–62
1224–6407	300°.0	−1°.4	4.3±1.4	11.4±0.7	4	1221–63
1326–5859	307°.5	3°.6	3.0	—	5	1323–58
1401–6357	310°.6	−2°.1	1.6±0.5	2.7±0.7	4	1358–63
1453–6413	315°.7	−4°.4	2.5±0.5	—	2	1449–64
1559–4438	334°.5	6°.4	2.0±0.5	—	2	1556–44
1600–5044	330°.7	1°.6	6.4±0.5	18.2±1.2	6	1557–50
1602–5100	330°.7	1°.3	7.4±0.5	9.4±0.4	6	1558–50
1651–4246	342°.5	0°.9	4.8±0.3	—	3	1648–42
1707–4053	345°.7	−2°.2	3.8±0.5	—	3	1703–40
1709–4429	343°.1	−2°.7	2.4±0.6	3.2±0.4	2	1706–44
1721–3532	351°.7	0°.7	4.4±0.5	5.2±0.6	3	1718–35
1740–3015	358°.3	0°.2	—	5.5±0.6	6	1737–30
1745–3040	358°.6	−1°.0	—	5.5±0.6	6	1742–30
1801–2305	6°.8	−0°.1	3.5	6.9	1	1758–23
1824–1945	12°.3	−3°.1	3.2±0.5	—	6	1821–19
1825–0935	21°.5	1°.3	—	1.9±0.4	6	1822–09
1833–0827	23°.4	0°.1	4.0±0.4	5.3±0.3	3	1830–08

References: 1 - Frail et al. (1993), 2 - Paper I, 3 - Weisberg et al. (1995), 4 - Paper II, 5 - Saravanan et al. (1996), 6 - this paper.

Figure 1. HI spectra in the direction of seven southern pulsars. The pulsar name (J2000) is given on top of each plot. Each panel shows the HI emission spectrum on top, the weighted HI absorption spectrum in the middle, and the corresponding part of the Galaxy rotation curve on the bottom. See the text for further description.



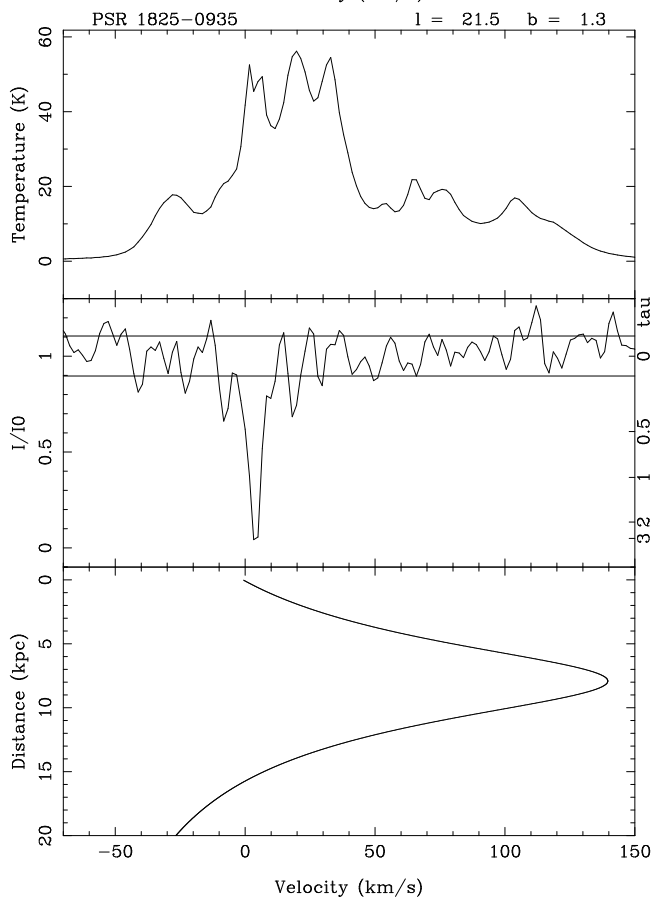
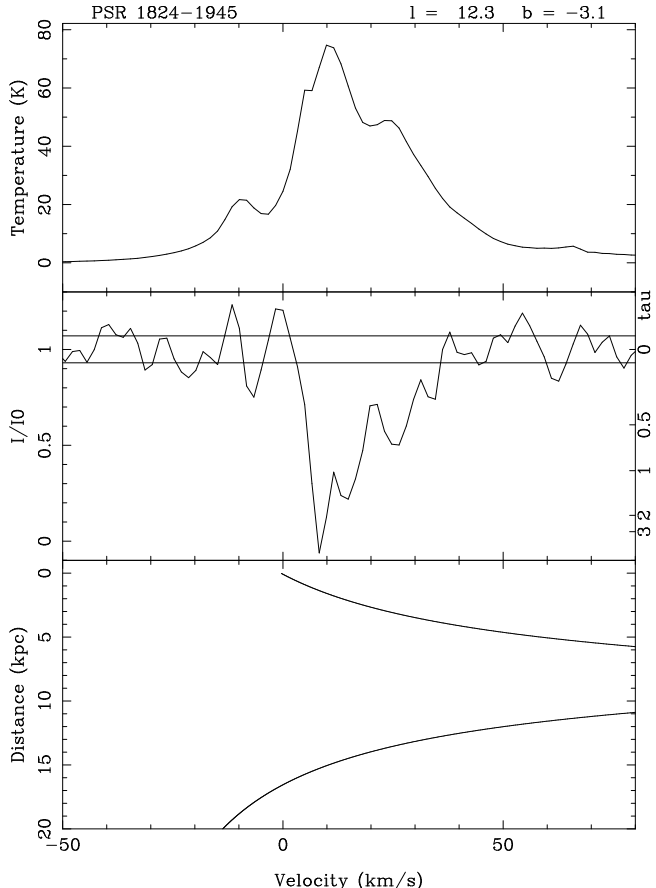
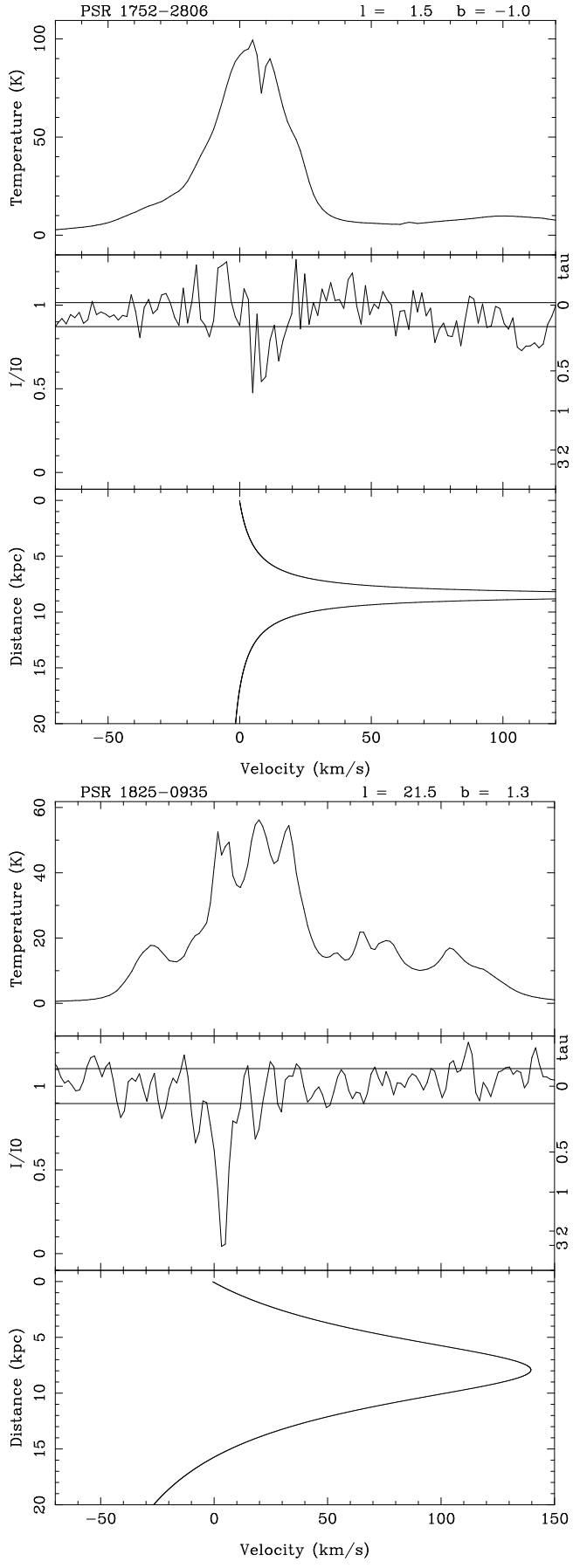


Figure 2. Distance limits on 24 mostly inner Galaxy pulsars measured since the Taylor & Cordes (1993) model was created. The ends of each line represent the upper and lower limits along a particular line of sight, while the diamond shows the model-estimated distance. An arrowhead on the end of a bar indicates that no upper distance limit was determinable. The thick curves show the location of the four spiral arms as delineated by Taylor & Cordes; from top to bottom the Perseus arm, the Sagittarius-Carina arm, the Scutum-Crux arm and the Norma arm. We also show the inner annulus of enhanced electron density derived in their model. See Table 3 for details on the individual pulsars plotted here.

